



## Research Paper

# The highly stable aqueous solution of sodium dodecahydro-*closos*-dodecaborate $\text{Na}_2\text{B}_{12}\text{H}_{12}$ as a potential liquid anodic fuel



Sergii Pylypko<sup>a</sup>, Salem Ould-Amara<sup>a</sup>, Anicet Zadick<sup>b,c</sup>, Eddy Petit<sup>a</sup>, Marian Chatenet<sup>b,c,d</sup>, Marc Cretin<sup>a</sup>, Umit B. Demirci<sup>a,\*</sup>

<sup>a</sup> IEM (Institut Européen des Membranes), UMR 5635, Université de Montpellier, CNRS, ENSCM, Place Eugène Bataillon, CC047, F-34095, Montpellier, France

<sup>b</sup> Univ. Grenoble Alpes, LEPMI, F-38000 Grenoble, France

<sup>c</sup> CNRS, LEPMI, F-38000 Grenoble, France

<sup>d</sup> Member of the French University Institute, Paris, France

## ARTICLE INFO

## ABSTRACT

## Keywords:

Borane  
Oxidation  
Polyborane  
Sodium dodecahydro-*closos*-dodecaborate  
( $\text{Na}_2\text{B}_{12}\text{H}_{12}$ )  
Platinum  
Gold

Herein are reported the first results and the discussion about the oxidation of the highly stable aqueous solution of sodium dodecahydro-*closos*-dodecaborate  $\text{Na}_2\text{B}_{12}\text{H}_{12}$ , a potential anodic fuel for energy conversion devices (fuel cells). The anion  $\text{B}_{12}\text{H}_{12}^-$  is indeed chemically stable: it has an excellent stability over 3 weeks in both alkaline and acidic media; and heterogeneous hydrolysis does not take place as evidenced by differential electrochemical mass spectrometry (DEMS) measurements (using a gold electrode). According to the cyclic voltammetry experiments, the  $\text{B}_{12}\text{H}_{12}^{2-}$  anion can be oxidized over bulk electrodes made of platinum, gold or silver, the oxidation taking place at low potential values with platinum and high potential values with gold and silver electrodes. The overall reaction is complex and generates various products, which were analyzed over 1000 cycles of voltammetry in the range –1.05 and 0.6 V vs. SCE. These products are mainly composed of  $\text{B}_7$ - and  $\text{B}_{11}$ -based polyboranes, which is indicative of a partial oxidative degradation of  $\text{B}_{12}\text{H}_{12}^-$ . To sum up, the present article demonstrates the potential of the aqueous solution of sodium dodecahydro-*closos*-dodecaborate  $\text{Na}_2\text{B}_{12}\text{H}_{12}$  as anodic fuel, but it also stresses on the necessity of further works especially focusing on multi-metallic electrodes (electrocatalysts) that could quantitatively and completely valorize this fuel.

## 1. Introduction

Within the past two decades, boron hydrides have shown to be potential (i) materials for liquid- and/or solid-state chemical hydrogen storage and (ii) liquid anodic fuels of direct liquid fuel cells. Boron hydrides draw their strong potential from the hydridic hydrogen elements  $\text{H}^-$ . (i) They react with protic hydrogen atoms  $\text{H}^+$  (e.g. from water) to generate  $\text{H}_2$  ( $\text{H}^- + \text{H}^+ \rightarrow \text{H}_2$ ), and (ii) they can be oxidized in alkaline medium with generation of 2 electrons ( $\text{H}^- \rightarrow \text{H}^+ + 2\text{e}^-$ ) while the as-formed  $\text{H}^+$  concomitantly react with  $\text{OH}^-$  towards the formation of  $\text{H}_2\text{O}$ . One can thus readily understand the potential of such hydrides in the field of new/alternative energies [1,2].

A first example of the aforementioned boron hydrides is sodium borohydride  $\text{NaBH}_4$ . It has a good solubility in water (55 g in 100 g  $\text{H}_2\text{O}$ ). It is not stable when the pH is below 7–8, due to the occurrence of self-hydrolysis ( $\text{BH}_4^- + 4\text{H}_2\text{O} \rightarrow \text{B}(\text{OH})_4^- + 4\text{H}_2$ ), but in alkaline conditions (pH = 9–12) the stability is drastically improved and can be considered near-perfect above pH = 13 [3–5]. Aqueous alkaline

solution of  $\text{NaBH}_4$  is then suitable for the generation of electrons by (electrochemical) oxidation. The borohydride oxidation reaction (the so-called BOR:  $\text{BH}_4^- + 8\text{OH}^- \rightarrow \text{BO}_2^- + 6\text{H}_2\text{O} + 8\text{e}^-$ ) was first reported in 1953 [6]. The standard potential of the reaction is –1.24 V vs. the reversible hydrogen electrode (RHE) [7], which is ca. 0.4 V below that for  $\text{H}_2$  oxidation (pH = 14). This explains why in the past two decades, the borohydride oxidation reaction has been widely investigated for electrochemical energy conversion purposes [8–11] or for its interest as a strong reducing agent in metal deposition or chemical synthesis [12]. The following aspects, which are related to the main issues of using  $\text{NaBH}_4$  as a strong reducer/fuel, have been especially investigated: electro-catalyst/catalysis of the BOR, features of the aqueous alkaline solution, membrane and crossover of ions, hydrolysis and oxidation mechanisms, and cathode (fuel and electro-catalyst) (see e.g. [11] for details).

A second example of boron hydride is the adduct ammonia borane  $\text{NH}_3\text{BH}_3$ . It is soluble in water (35 g in 100 g  $\text{H}_2\text{O}$ ) and satisfactorily stable when the pH is 7 or above [13]. Within the past two decades, the

\* Corresponding author.

E-mail address: [umit.demirci@umontpellier.fr](mailto:umit.demirci@umontpellier.fr) (U.B. Demirci).

oxidation of this compound ( $\text{NH}_3\text{BH}_3 + 6\text{OH}^- \rightarrow \text{NH}_4^+ + \text{BO}_2^- + 4\text{H}_2\text{O} + 6\text{e}^-$ ; standard potential of  $-1.22\text{ V}$  vs. RHE) has been scarcely studied [14–19]. In fact,  $\text{NH}_3\text{BH}_3$  and  $\text{NaBH}_4$  suffer from the same main issues (e.g. the occurrence of heterogeneous hydrolysis with evolution of the unwanted  $\text{H}_2$ ). However,  $\text{NaBH}_4$  is superior in terms of theoretical (and usually also of effective) number of electrons exchanged (6 vs. 8 respectively), and  $\text{NH}_3\text{BH}_3$  is synthesized from  $\text{NaBH}_4$  making it more expensive [20]; both points explain why the development of aqueous  $\text{NH}_3\text{BH}_3$  as liquid anodic fuel remains limited in comparison to  $\text{NaBH}_4$ .

More recently, a third example of boron hydride, sodium octahydrotriborate  $\text{NaB}_3\text{H}_8$ , has been reported [21]. It is much soluble in water (74 g in 100 g  $\text{H}_2\text{O}$ ), even more soluble than  $\text{NaBH}_4$ , but the aqueous solution of  $\text{NaB}_3\text{H}_8$  is comparable to the aqueous solution of  $\text{NaBH}_4$  in terms of stability even in alkaline conditions. In solution, the  $\text{B}_3\text{H}_8^-$  anion transforms into the  $\text{BH}_4^-$  anion and the latter readily hydrolyzes. Regardless of that,  $\text{NaB}_3\text{H}_8$  is a possible liquid anodic fuel. Theoretically, the oxidation is expected to release 18 electrons ( $\text{B}_3\text{H}_8^- + 20\text{OH}^- \rightarrow 3\text{BO}_2^- + 14\text{H}_2\text{O} + 18\text{e}^-$ ; standard potential of the reaction not available). Experimentally, the effective number of electrons is 10 electrons with a gold electrode, the authors pointing out that gold may not be the proper electrocatalyst to valorize  $\text{B}_3\text{H}_8^-$ . Incomplete oxidation is due to the occurrence of heterogeneous hydrolysis (and  $\text{H}_2$  evolution).

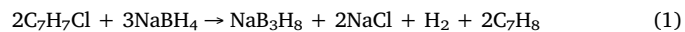
As mentioned above, the oxidations of  $\text{NaBH}_4$ ,  $\text{NH}_3\text{BH}_3$  and  $\text{NaB}_3\text{H}_8$  suffer from several problems relating to the aqueous solution properties, the electrocatalyst (nature and texture), the membrane and so forth. Two aspects are particularly problematic: the instability of the boron hydride in water (mainly in the case of  $\text{NaBH}_4$  and  $\text{NaB}_3\text{H}_8$ ) and the nature of the borate by-product ( $\text{BO}_2^-$  for the anhydrous form and the  $\text{B(OH)}_4^-$  for the hydrated compound). The former issue has been briefly discussed in the previous paragraphs. The latter issue is inherent to the high stability of the B–O bonds, which is comparable to that of the C=O bonds in carbon dioxide  $\text{CO}_2$ . The recycling of  $\text{BO}_2^-$  with regeneration of  $\text{NaBH}_4$  is thermodynamically unfavorable and currently realized through costly processes [22]. Yet, it is pivotal to close the energy cycle with boron hydrides for a possible near-future technological deployment. Breakthrough in the recycling of borates is evidently required.

Another strategy would be to circumnavigate the aforementioned challenges by envisaging alternative liquid anodic fuels, and it was chosen to explore this strategy. The chemistry of boranes has a history going back one century: it has given rise to a very great number of molecules, from diborane  $\text{B}_2\text{H}_6$  to polyhedral boranes. Polyhedral boranes have been widely used in medical and pharmacological applications owing to their exceptional stability (low chemical reactivity and resistance to breakdown in biological systems) rendering them relatively nontoxic [23,24]. For the present work, a polyhedral borane anion salt, namely sodium dodecahydro-closo-dodecaborane  $\text{Na}_2\text{B}_{12}\text{H}_{12}$ , was selected. It has a good solubility in water, is stable in aqueous solution, is comparable to sodium chloride  $\text{NaCl}$  in terms of nontoxicity, and is less sensitive to catalytic hydrolysis than other polyhedral borane anions like  $\text{B}_{10}\text{H}_{10}^{2-}$  and  $\text{B}_{11}\text{H}_{14}^-$  [24,25]. Accordingly, is reported herein, for the first time, preliminary results about the oxidation of aqueous  $\text{Na}_2\text{B}_{12}\text{H}_{12}$  on bulk electrodes (platinum, gold, or silver) as well as a discussion about its potential as liquid anodic fuel.

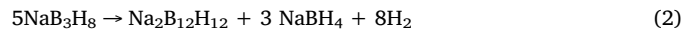
## 2. Experimental

The synthesis of  $\text{Na}_2\text{B}_{12}\text{H}_{12}$  was performed according to a new multi-step procedure, actually adapted from previous reports [26,27]. The manipulations were performed under argon. Standard Schlenk-line and glove box (MBraun M200B;  $\text{O}_2 < 0.1\text{ ppm}$ ;  $\text{H}_2\text{O} < 0.1\text{ ppm}$ ) techniques were used. In a three-necked round-bottom flask equipped with a condenser, 20 g of  $\text{NaBH}_4$  ( $\geq 98\%$ , Sigma-Aldrich) were

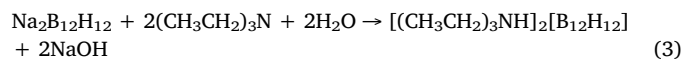
dispersed in 350 mL anhydrous diglyme  $\text{C}_6\text{H}_{14}\text{O}_3$  ( $\geq 99\%$ , Sigma-Aldrich) and heated up to  $100\text{ }^\circ\text{C}$ . Using an addition funnel, 50 mL of benzyl chloride  $\text{C}_7\text{H}_7\text{Cl}$  ( $\geq 99\%$ , Sigma-Aldrich) was slowly added to the  $\text{NaBH}_4$  dispersion.  $\text{NaB}_3\text{H}_8$  formed ( $^{11}\text{B}$  NMR ( $96.29\text{ MHz}$ ,  $\text{CD}_3\text{CN}$ )  $\delta -30.6\text{ ppm}$  (nonet);  $^1\text{H}$  NMR ( $300.13\text{ MHz}$ ,  $\text{CD}_3\text{CN}$ ):  $\delta 0.2\text{ ppm}$  (decet)) [21]:



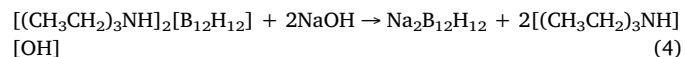
Upon the completion of this reaction, the temperature was increased to  $165\text{ }^\circ\text{C}$ .  $\text{NaB}_3\text{H}_8$  decomposed:



The reaction mixture was kept at  $165\text{ }^\circ\text{C}$  overnight. Then, the solvent was extracted at  $140\text{ }^\circ\text{C}$  under vacuum. The setup was cooled down to room temperature and the drying was completed under dynamic vacuum at  $-47\text{ }^\circ\text{C}$ . A yellowish solid consisting of mainly  $\text{Na}_2\text{B}_{12}\text{H}_{12}$  and  $\text{NaBH}_4$  was obtained. For purification, the solid was dissolved in 150 mL of Milli-Q water ( $18.2\text{ M}\Omega\text{ cm}$ ) and 60 mL of hydrochloric acid  $\text{HCl}$  (36.5–38%, Sigma-Aldrich). The additions were done very slowly because of the evolution of  $\text{H}_2$  by acid attack of  $\text{NaBH}_4$  ( $\text{Na}_2\text{B}_{12}\text{H}_{12}$  is stable in acidic medium). Boric acid  $\text{B(OH)}_3$  formed. It was crystallized by storing the solution at  $-6\text{ }^\circ\text{C}$  overnight. The as-formed crystals were filtrated. Then, about 50 mL of triethylamine  $(\text{CH}_2\text{CH}_3)_3\text{N}$  ( $\geq 99\%$ , Sigma-Aldrich) was added to the acidic aqueous solution to increase the pH up to 9–10. The as-obtained alkaline solution was stirred overnight. A white precipitate formed:



It was collected by filtration and dried under dynamic vacuum at ambient temperature. The remaining traces of boric acid were removed by dissolution with 50 mL of Milli-Q water at  $60\text{ }^\circ\text{C}$ . Purified  $[(\text{CH}_3\text{CH}_2)_3\text{NH}]_2[\text{B}_{12}\text{H}_{12}]$  was recovered after filtration. As a last step, cation substitution was performed by interaction with sodium hydroxide  $\text{NaOH}$  ( $\geq 98\%$ , BioXtra) in Milli-Q water:



By this way, 3.6 g of a white solid consisting of  $\text{Na}_2\text{B}_{12}\text{H}_{12}$  was recovered (yield of 43.5%).

Nuclear magnetic resonance (NMR) was used for the structural analysis of  $\text{Na}_2\text{B}_{12}\text{H}_{12}$  in solution: nuclei  $^1\text{H}$  and  $^{13}\text{C}$  (probe head dual  $^1\text{H}/^{13}\text{C}$ ,  $300.13\text{ MHz}$ ,  $\text{CD}_3\text{CN}$ ,  $30\text{ }^\circ\text{C}$ ); nucleus  $^{11}\text{B}\{^1\text{H}\}$  (probe head BBO10,  $96.29\text{ MHz}$ ,  $\text{D}_2\text{O}$ ,  $30\text{ }^\circ\text{C}$ ); apparatus Bruker AVANCE-300. Analyses by Fourier transform infrared (FTIR; Nicolet 710, 128 scans) and Raman spectroscopy techniques were also performed. For the latter technique, the measurements were carried out using a confocal microspectrometer (Labram HR, Jobin-Yvon) with the sample in a sealed glass tube kept at  $25\text{ }^\circ\text{C}$  (diode laser beam  $659.55\text{ nm}$ ). Powder X-ray diffraction (PXRD) was carried out on a PANalytical X'Pert diffractometer equipped with an X'Celerator detector. The  $2\theta$  range was between 10 and  $50\text{ }^\circ$ . Pattern matching was performed using the EVA software and available crystallographic databases (PDF-4+ v. 4.1403). Thermogravimetric analysis (TGA) of  $\text{Na}_2\text{B}_{12}\text{H}_{12}$  was performed with the apparatus TGA Q500 of TA Instruments. Typically,  $\sim 3\text{ mg}$  of solid was introduced into an aluminum crucible ( $40\text{ }\mu\text{L}$ ) and then heated up to  $400\text{ }^\circ\text{C}$  at  $5\text{ min}^{-1}$  under  $\text{N}_2$  flow ( $60\text{ mL min}^{-1}$ ). The same experimental conditions were applied for analysis by differential scanning calorimetry (DSC; apparatus: 2920 MDSC of TA Instruments).

Cyclic voltammetry (CV) experiments were performed with a  $\mu\text{Autolab}^*$  Type III potentiostat using a three-electrode cell. Saturated calomel electrode (SCE, the reference potential of which is  $0.241\text{ V}$  vs. SHE, i.e.  $1.008\text{ V}$  vs. RHE,  $\text{pH} = 13$ ) was used as reference electrode and platinum wire as counter electrode. Gold ( $\phi 1\text{ mm}$ ), platinum ( $\phi 1\text{ mm}$ ), silver ( $\phi 2\text{ mm}$ ) and glassy carbon ( $\phi 2\text{ mm}$ ) were used as

rotating disk working electrode. Outgassed Milli-Q Water ( $18.2 \text{ M}\Omega \text{ cm}$ ,  $< 3 \text{ ppb}$  total organic carbon) was systematically used to prepare the electrolyte solutions. Prior to any new experiment, the glassware and electrodes were treated with a peroxymonosulfuric acid  $\text{H}_2\text{SO}_5$  (Caro's acid) overnight and carefully washed with Milli-Q water, and the surface of the working electrodes were polished with diamond paste. The cell was degassed with argon to avoid  $\text{O}_2$  reduction and carbonation of the electrolyte from ambient  $\text{CO}_2$ . The cell was systematically thermostated at  $20^\circ\text{C}$ . The voltage range was fixed:  $-1.05$  to  $+0.6 \text{ V vs. SCE}$  (in order to avoid water splitting). The electrolyte had the following features: alkaline ( $0.1 \text{ M NaOH}$ ) aqueous solution of  $\text{Na}_2\text{B}_{12}\text{H}_{12}$  ( $0.001 \text{ M}$ ).

Differential electrochemical mass spectrometry (DEMS; Pfeiffer Vacuum QMA 200 quadrupole mass spectrometer) measurements were performed to detect  $\text{H}_2$  at different electrochemical potentials (cycling from  $-1.05$  to  $0.6 \text{ V vs. SCE}$ ; scan rate of  $10 \text{ mV s}^{-1}$ ; PGSTAT 302N potentiostat from Autolab). The spectrometer was coupled to an electrochemical cell for online measurements. The technique is described in detail elsewhere [28]. The DEMS setup consists of two differentially pumping chambers. The electrochemical cell, Pyrex-based, is hermetically fixed to a differential vacuum compartment (creating a cascade of vacuum from *ca.*  $10^{-3} \text{ mbar}$  in the primary chamber just below the working electrode, all the way to *ca.*  $10^{-6} \text{ mbar}$  in the MS chamber); it bares five inputs for the three electrodes (working, counter and reference), the argon bubbling (inlet) and an additional one for the argon outlet. The working electrode is a gold film sputtered onto a Gore-Tex® PTFE membrane; its porous nature enables the detection of the volatile and/or gaseous products during electrochemistry. During the analysis, the gases, if any, are pumped through the PTFE membrane to be analyzed by the mass spectrometer. The electrochemical data are recorded along with the  $m/z$  signals, especially  $m/z = 2$  for  $\text{H}_2$ .

Additional analysis of the oxidation by-products (in solution) was performed by mass spectrometry (MS). The apparatus was as follows: Waters Micromass (Wytenshaw, Manchester, UK) Quattro Micro mass spectrometer with an electrospray ionization in negative mode (ESI). Analysis were done in direct injection (FIA: Flow Injection Analysis) by a Waters 2695 pump-autosampler with  $20 \mu\text{L}$  loop. The mobile phase was a 50/50 (vol.%) mixture of water and acetonitrile (both of HPLC grade). The flow rate to the spectrometer was constant at  $0.25 \text{ mL min}^{-1}$ . The detection conditions were as follows: capillary potential  $3.5 \text{ kV}$ ; cone potential  $30 \text{ V}$ ; source temperature  $120^\circ\text{C}$ ; desolvation temperature  $450^\circ\text{C}$ ; cone gas flow  $50 \text{ L h}^{-1}$ ; desolvation gas flow  $450 \text{ L h}^{-1}$ . Nitrogen was used as the nebulizer gas. The analysis conditions were in fact optimized with the help of the fresh electrolyte ( $0.1 \text{ M NaOH}$  aqueous solution of  $0.001 \text{ M Na}_2\text{B}_{12}\text{H}_{12}$ ) to ensure that the  $\text{B}_{12}\text{H}_{12}^{2-}$  anion did not degrade. The optimization mainly concerned the cone potential; it was varied from  $5$  to  $120 \text{ V}$ ; it was observed (*via* high resolution measurements) no degradation below  $30 \text{ V}$ . The technique is not quantitative because of the discrepancies in the ionization yield of the molecules, however the technique is efficient in detecting the nature of the oxidation products by their isotopic peak profile.

### 3. Results and discussion

#### 3.1. Sodium dodecahydro-closo-dodecaborane $\text{Na}_2\text{B}_{12}\text{H}_{12}$

The successful synthesis of  $\text{Na}_2\text{B}_{12}\text{H}_{12}$  was first verified by NMR. The  $^1\text{H}$  NMR spectrum (Fig. 1a) is characterized by several signals. The large multiplet in the  $0$ – $1.9 \text{ ppm}$  region is attributed to the  $\text{BH}$  resonance. The signal is complex due to heteronuclear coupling between  $^{11}\text{B}$  and  $^1\text{H}$  as well as heteronuclear coupling between  $^{10}\text{B}$  and  $^1\text{H}$ . Acetonitrile  $\text{CH}_3\text{CN}$  and water  $\text{H}_2\text{O}$  contained in the deuterated solvent shows the signals of very high intensity at  $1.95$  and  $2.35 \text{ ppm}$ . There are several other signals of small intensity ( $2.2$ ,  $2.4$ ,  $3.2$  and  $3.5 \text{ ppm}$ ); unidentified impurities may explain the presence of the other small

signals. The  $^{11}\text{B}\{^1\text{H}\}$  NMR spectrum of aqueous  $\text{Na}_2\text{B}_{12}\text{H}_{12}$  (Fig. 1b) shows a doublet centered at  $-15.9 \text{ ppm}$  with a  $^{1}\text{J}_{\text{B}-\text{H}}$  coupling constant of  $124.7 \text{ Hz}$ . It is typical of the 12 equivalent boron atoms constituting the boron skeleton of the anion  $\text{B}_{12}\text{H}_{12}^{2-}$  [29]. No other boron-containing compound was detected.

The FTIR (Fig. 1c) and Raman spectra (Fig. 1d) of  $\text{Na}_2\text{B}_{12}\text{H}_{12}$  are consistent with previous reports [27,30,31]. The FTIR spectrum shows 6 main vibration modes that can be ascribed as follows:  $3640$ – $3340 \text{ cm}^{-1}$  for O–H stretching;  $2560$ – $2200 \text{ cm}^{-1}$  for B–H (symmetric/asymmetric) stretching;  $1610 \text{ cm}^{-1}$  for O–H bending;  $1074 \text{ cm}^{-1}$  for vibration of a B–B bond of the boron cage;  $713$  and  $532 \text{ cm}^{-1}$  for B–H bending/rocking vibrations. The O–H bending mode is an indication of the presence of structural water [31]. The Raman spectrum shows the same vibrational modes, except for water which is a fairly weak Raman scatterer.

$\text{Na}_2\text{B}_{12}\text{H}_{12}$  is a crystalline white solid (Fig. 2). It favorably compares to the PXRD pattern of the pure compound reported elsewhere [32,33], then confirming a monoclinic crystal structure with a space group  $P2_1/n$ . Yet, there are some differences and all of the diffraction peaks can be ascribed only by considering the presence of a hydrated form of  $\text{Na}_2\text{B}_{12}\text{H}_{12}$ . Pattern matching suggested the presence of the dihydrated structure  $\text{Na}_2\text{B}_{12}\text{H}_{12}\cdot 2\text{H}_2\text{O}$  (ICDD 00-045-0789).

The thermal stability of  $\text{Na}_2\text{B}_{12}\text{H}_{12}$  was investigated by TGA and DSC (Fig. 3). Our sample is stable up to  $61^\circ\text{C}$ , then it losses  $2.6 \text{ wt\%}$  over the range  $61$ – $145^\circ\text{C}$ . This is characterized by 2 successive endothermic signals. The solid heated up to  $150^\circ\text{C}$  was analyzed by  $^{11}\text{B}\{^1\text{H}\}$  NMR (Fig. 1b) and the structural stability of  $\text{Na}_2\text{B}_{12}\text{H}_{12}$  was confirmed. It is assumed that the weight loss at  $< 100^\circ\text{C}$  is due to surface water and that at  $> 100^\circ\text{C}$  to structural water [32]. This is in agreement with the FTIR and PXRD data. At higher temperature ( $258^\circ\text{C}$ ), an additional endothermic signal accompanied with a very low mass loss ( $0.3 \text{ wt\%}$ ) can be observed. This is explained by a hysteretic phase transition [33]. Anhydrous  $\text{Na}_2\text{B}_{12}\text{H}_{12}$  is known to be stable up to  $580^\circ\text{C}$  (dehydrogenation) [32]. Hence, the overall weight loss between  $61$  and  $315^\circ\text{C}$  ( $2.9 \text{ wt\%}$  of  $\text{H}_2\text{O}$ ) allows calculating the mean formulae of our synthesized sample. It would be  $\text{Na}_2\text{B}_{12}\text{H}_{12}\cdot 0.25\text{H}_2\text{O}$ , suggesting on the basis of the PXRD results a mixture of  $\text{Na}_2\text{B}_{12}\text{H}_{12}$  and  $\text{Na}_2\text{B}_{12}\text{H}_{12}\cdot 2\text{H}_2\text{O}$  (hypothetical mole ratio of 7:1).

The stability of  $\text{Na}_2\text{B}_{12}\text{H}_{12}$  in alkaline ( $0.1$  and  $1 \text{ M NaOH}$ ) and acidic ( $0.05$  and  $0.5 \text{ H}_2\text{SO}_4$ ) aqueous solutions was studied. The fresh solutions were first analyzed by  $^{11}\text{B}\{^1\text{H}\}$  NMR. They were stored for 3 weeks, then analyzed again by  $^{11}\text{B}\{^1\text{H}\}$  NMR (Fig. 4). Whatever the pH of the aqueous solutions, the anion  $\text{B}_{12}\text{H}_{12}^{2-}$  is not affected, which evidences the remarkable stability of the compound in neutral, basified and acidified water [30,34]. Unlike for  $\text{NaBH}_4$ ,  $\text{NH}_3\text{BH}_3$  and  $\text{NaB}_3\text{H}_8$ , hydrolysis and/or acidic attack do not take place, which is an attractive feature for a boron-based liquid anodic fuel.

Before the cyclic voltammetry (CV) experiments, the possible occurrence of heterogeneous hydrolysis [28] of the anion  $\text{B}_{12}\text{H}_{12}^{2-}$  (*i.e.* evolution of  $\text{H}_2$ ) was studied by differential electrochemical mass spectrometry on a sputtered gold electrode (DEMS, Fig. 5). Two alkaline ( $0.1 \text{ M NaOH}$ ) aqueous solutions of  $\text{B}_{12}\text{H}_{12}^{2-}$  ( $0.001$  and  $0.05 \text{ M}$ ) were prepared. The experiments started with the aqueous solution of  $\text{NaOH}$  ( $0.1 \text{ M}$ ; borane-free supporting electrolyte). The time variation of the open circuit potential along with the evolution of  $\text{H}_2$  was monitored: the potential of the gold electrode remained constant at  $-0.16 \text{ V vs. SCE}$  in the supporting electrolyte. Then,  $\text{B}_{12}\text{H}_{12}^{2-}$  was added to obtain a  $0.001 \text{ M}$   $\text{B}_{12}\text{H}_{12}^{2-}$  solution. A negative shift of the gold electrode potential was observed ( $-0.22 \text{ V vs. SCE}$ ) because of the reducing character of the borane, but no  $\text{H}_2$  was detected. The data were collected for  $1.5 \text{ h}$ . Then, another addition of  $\text{B}_{12}\text{H}_{12}^{2-}$  was made to reach the  $0.05 \text{ M}$   $\text{B}_{12}\text{H}_{12}^{2-}$  solution. As expected, a further negative shift of the electrode potential was observed ( $-1.1 \text{ V vs. SCE}$ ), but still no evolution of  $\text{H}_2$  was detected in these conditions. Finally, an additional test was done, by carrying out a CV experiment while analyzing

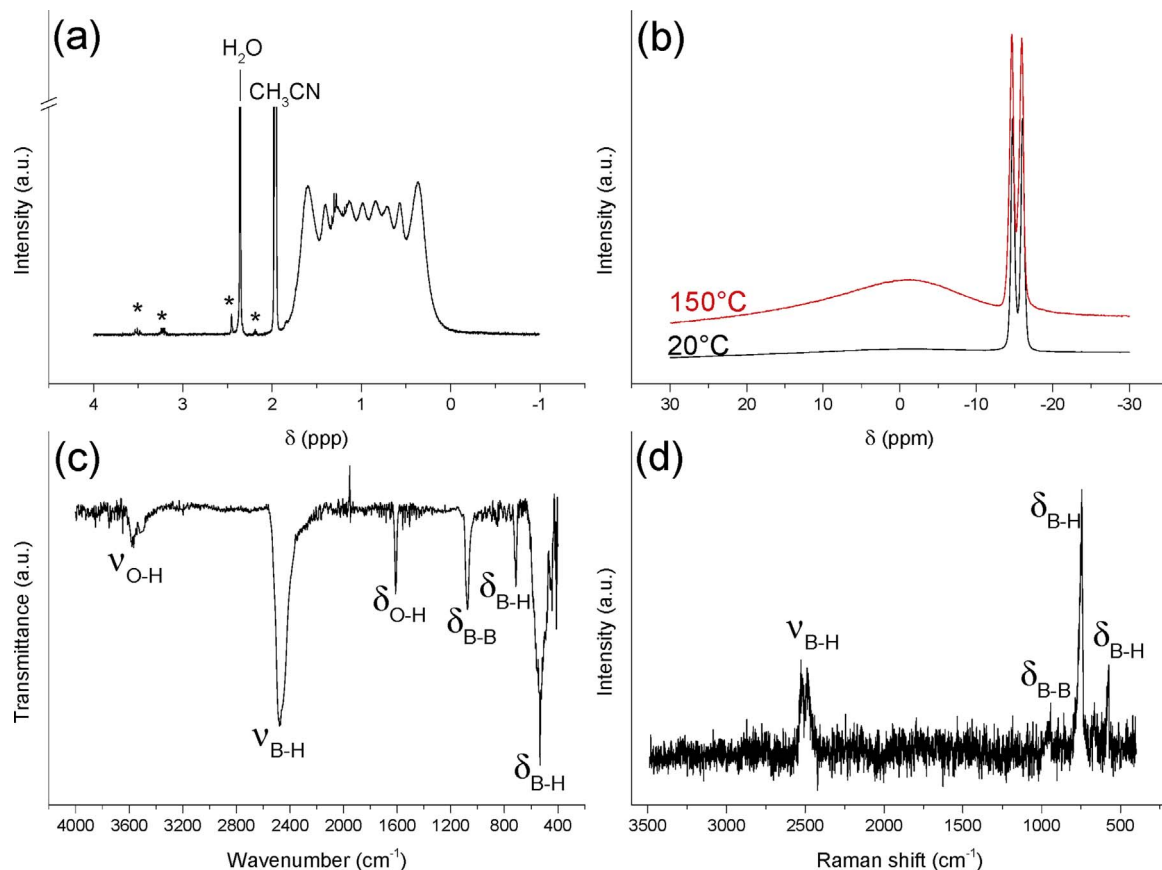


**Fig. 1.** (a)  $^1\text{H}$  NMR spectrum of  $\text{Na}_2\text{B}_{12}\text{H}_{12}$  (the stars indicate the impurities); (b)  $^{11}\text{B}\{^1\text{H}\}$  NMR spectrum of fresh  $\text{Na}_2\text{B}_{12}\text{H}_{12}$  and heat-treated (at 150 °C)  $\text{Na}_2\text{B}_{12}\text{H}_{12}$ ; (c) FTIR and (d) Raman spectra of  $\text{Na}_2\text{B}_{12}\text{H}_{12}$ .

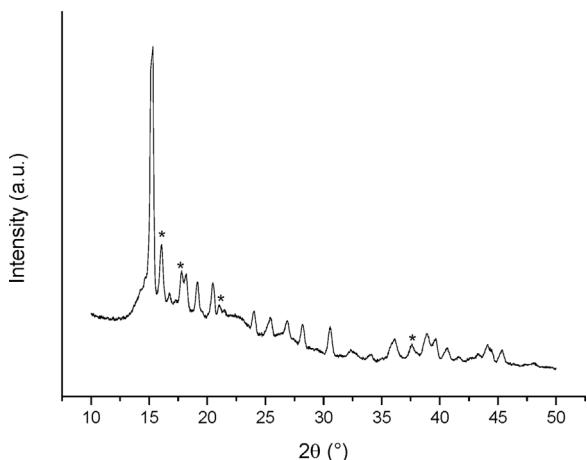


**Fig. 2.** XRD pattern of  $\text{Na}_2\text{B}_{12}\text{H}_{12}$ . The unmarked peaks are attributed to  $\text{Na}_2\text{B}_{12}\text{H}_{12}$  while the stars show the peaks ascribed to  $\text{Na}_2\text{B}_{12}\text{H}_{12}\cdot 2\text{H}_2\text{O}$  (ICDD 00-045-0789).

any evolving gas (Fig. 6). No hydrogen was detected on the whole potential range investigated, even though the gold electrode presents a clear activity with regards to the oxidation of  $\text{B}_{12}\text{H}_{12}^{2-}$ . This is a further evidence of the absence of heterogeneous hydrolysis of  $\text{B}_{12}\text{H}_{12}^{2-}$  on a gold electrode.

### 3.2. Oxidation of $\text{Na}_2\text{B}_{12}\text{H}_{12}$

As a preliminary CV experiment, the inertness of  $\text{B}_{12}\text{H}_{12}^{2-}$  on the glassy carbon electrode was confirmed: whatever the conditions of mass-transfer, the same CV is monitored, which shows the absence of

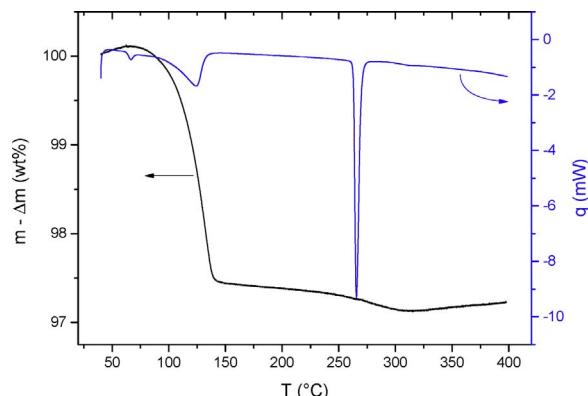


**Fig. 3.** TGA (in black) and DSC (in blue) curves of  $\text{Na}_2\text{B}_{12}\text{H}_{12}$  ( $40\text{--}400\text{ }^\circ\text{C}$ ;  $5\text{ }^\circ\text{C min}^{-1}$ ,  $\text{N}_2$  flow). (For interpretation of the references to colour in this figure legend, the reader is referred to the web version of this article.)

any faradaic current (Fig. 7). Oxidation of  $\text{B}_{12}\text{H}_{12}^{2-}$  was then studied on three different materials (platinum, gold and silver), using the rotating disk electrode (RDE) setup, which enables to control the mass-transfer of the reactants. To the authors' knowledge, there are very few reports on the oxidation of  $\text{B}_{12}\text{H}_{12}^{2-}$ . Kaczmarczyk et al. [35] investigated the oxidative degradation of several polyhedral boranes (including the  $\text{B}_{12}\text{H}_{12}^{2-}$  anion) into boric acid in the presence of the permanganate anion  $\text{MnO}_4^-$ . Wiersema and Middaugh [36] worked on the one-electron electrochemical oxidation (electrolysis) of  $\text{B}_{12}\text{H}_{12}^{2-}$  in acetonitrile. The anion  $\text{B}_{24}\text{H}_{23}^{3-}$  formed by connection of two reactants via a hydrogen bridge. Volkov et al. [37] performed the controlled oxidation of  $\text{B}_{12}\text{H}_{12}^{2-}$  in the presence of  $\text{Ag}^{2+}$  as a strong one-electron acceptor ( $E^\circ(\text{Ag}^{2+}/\text{Ag}^+) = 1.98\text{ V}$ ). A radical  $\text{B}_{12}\text{H}_{12}^{\cdot -}$  formed such

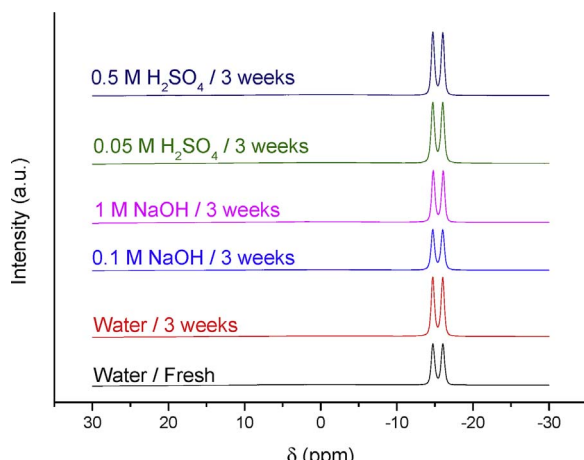


**Fig. 4.**  $^{11}\text{B}\{^1\text{H}\}$  NMR spectra of  $\text{Na}_2\text{B}_{12}\text{H}_{12}$  in aqueous solution at different pH values. The spectra were recorded after a storage of 3 weeks in: neutral water, alkaline solutions (0.1 and 1 M NaOH), and acidic solutions (0.05 and 0.5 M  $\text{H}_2\text{SO}_4$ ). The spectrum of fresh  $\text{Na}_2\text{B}_{12}\text{H}_{12}$  is also shown.

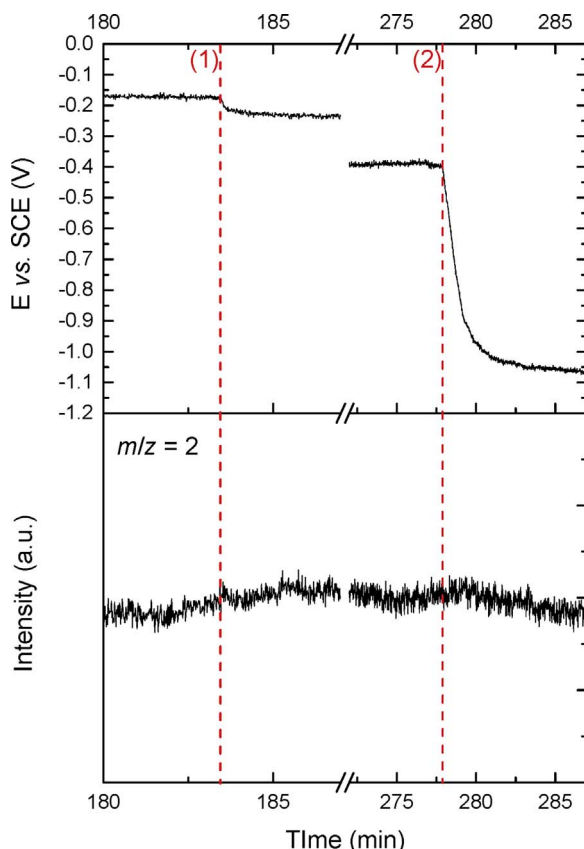
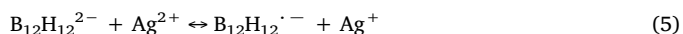


**Fig. 5.** Evolution of (top) the potential ( $E$  vs. SCE) as a function of time (in min), in parallel to (bottom) the evolution of the signal  $m/z = 2$  for  $\text{H}_2$  detected by DEMS as a function of time (in min), for a gold electrode. The additions of the solution 0.001 M  $\text{Na}_2\text{B}_{12}\text{H}_{12}$  at (1) and then that of the solution 0.05 M  $\text{Na}_2\text{B}_{12}\text{H}_{12}$  at (2) are indicated by the dashed vertical lines.

as:



Then, the radical  $\text{B}_{12}\text{H}_{12}^{\cdot-}$  was found to react with  $\text{O}_2$  towards the formation of the anion  $\text{OB}_{11}\text{H}_{12}^-$ :



The oxidation product is less stable than the reactant, as it was slowly decomposed by  $\text{O}_2$ , overall resulting in the formation of stoichiometric amounts of  $\text{B(OH)}_3$ . In these works, there is no mention of the occurrence of heterogeneous hydrolysis, which is consistent with the observations made above.

Given the context briefly described above, the below-reported cyclic voltammetry results have been analyzed and discussed in the light of the literature dedicated to oxidation of the anions  $\text{BH}_4^-$  and  $\text{B}_3\text{H}_8^-$ . The discussion particularly focuses on the references [8,11,21,28,38–42].

The electrooxidation of  $\text{B}_{12}\text{H}_{12}^{2-}$  was first studied with the platinum electrode (Fig. 8a). The voltammogram shows two oxidations peaks during the forward step (the main peak,  $a_{\text{Pt}1}$ , is observed at  $-0.70$  V vs. SCE and a secondary peak,  $a_{\text{Pt}2}$ , at  $-0.59$  V vs. SCE) and one oxidation peak on the backward sweep ( $c_{\text{Pt}1}$  peaking at  $-0.72$  V vs. SCE). Peak  $a_{\text{Pt}1}$  initiates at ca.  $-1.0$  V vs. SCE (i.e. at the RHE potential) and is more symmetric in conditions of controlled mass-transfer (diffusion convection at an RDE; Fig. S1): in that case, the low-potential contribution (below  $-0.8$  V vs. SCE) is not observed (as for  $c_{\text{Pt}1}$ ), which could suggest that this low-potential contribution is due to the oxidation of molecular hydrogen ( $\text{H}_2$ ); indeed  $\text{H}_2$  cannot remain at the electrode surface in RDE configuration (it is expelled by the convective flux of electrolyte) and has already been oxidized or evacuated by diffusion in the backward sweep. In addition, peaks  $a_{\text{Pt}1}$  and  $a_{\text{Pt}2}$  are in the region of the adsorption/desorption of atomic hydrogen on platinum surface (see the CV in supporting electrolyte, dashed line on the figure). They may therefore be attributed to the  $\text{B}_{12}\text{H}_{12}^{2-}$  dissociative adsorption and oxidation of the adsorbed hydrogen  $\text{H}_{\text{ads}}$  (except for the low-potential contribution of  $a_{\text{Pt}1}$ , linked to the oxidation of  $\text{H}_2$ ). Some direct (partial) oxidation of  $\text{B}_{12}\text{H}_{12}^{2-}$  cannot be discarded, but shall not be major on the platinum electrode. There is no oxidation peak (and current) at more positive potential (in the platinum-oxides region), so the adsorbed  $\text{B}_{12}$ -intermediates would either remain on the platinum surface (platinum-oxides being then inactive towards any oxidation of  $\text{B}_{12}\text{H}_{12}^{2-}$ ) or desorb. In the backward scan, once the platinum-oxides have been reduced, the platinum electrode is “re-generated”, and some oxidation current is observed (peak  $c_{\text{Pt}1}$ ), the latter being probably due to the oxidation of the  $\text{H}_{\text{ads}}$  species mentioned above. The CV experiments performed with different rotation rates of the platinum rotating disk electrode (Fig. S1) confirm the peaks assignation. The voltammograms are similar than in natural diffusion, but the current density of the peaks decreases with the increase of the revolution rates of the RDE ( $9.4 \text{ mA cm}^{-2}$  at 0 rpm to  $6.8 \text{ mA cm}^{-2}$  at 2500 rpm), which indicates (i) that the oxidation reaction is not limited by mass-transfer (but on the contrary by a slow charge-transfer kinetics) and (ii) that the platinum electrode is prone by self-poisoning by the adsorbed boron-based intermediates of the oxidation, as now abundantly discussed in the  $\text{BH}_4^-$  literature [41,43,44]. This is also indicative of complex electrochemical mechanisms where the anion  $\text{B}_{12}\text{H}_{12}^{2-}$  would adsorb and partially decompose at the electrode surface, leading to slow reaction kinetics and incomplete oxidation (only some adsorbed intermediates would be capable to react, e.g.  $\text{H}_{\text{ads}}$ ). The increase of the rotation rate would therefore have two detrimental effects: (i) it favors the desorption of the weakly-adsorbed electroactive intermediates (decreased residence time) resulting in the subsequent drop of the current density and/or (ii) it increases the surface coverage of strongly-adsorbed intermediates resulting from the dissociative adsorption of  $\text{B}_{12}\text{H}_{12}^{2-}$ , and enhances the platinum electrode poisoning, thereby decreasing its apparent activity. Whatever the explanation, platinum alone is not an optimized catalyst for the oxidation of  $\text{B}_{12}\text{H}_{12}^{2-}$ .

With the gold electrode, the cyclic voltammogram (Fig. 8b) shows one oxidation ( $a_{\text{Au}1}$  peaking at  $+0.20$  V vs. SCE) during the forward step, and the oxidation process is purely not reversible. Besides, the rotation of the gold rotating disk electrode has a negative impact on the current density which decreases from  $4.3 \text{ mA cm}^{-2}$  at 0 rpm to  $2.2 \text{ mA cm}^{-2}$  at 2500 rpm (Fig. S2), such decrease being again ascribed

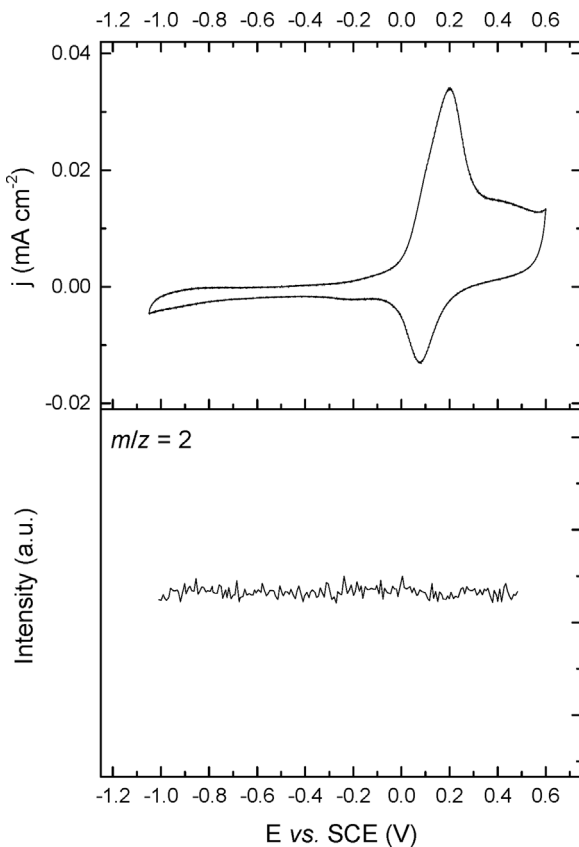


**Fig. 6.** Cyclic voltammogram (top) and evolution of the signal  $m/z = 2$  for  $\text{H}_2$  detected by DEMS (bottom) for the alkaline ( $0.1 \text{ M NaOH}$ ) aqueous solution of  $0.001 \text{ M Na}_2\text{B}_{12}\text{H}_{12}$  at gold electrode.

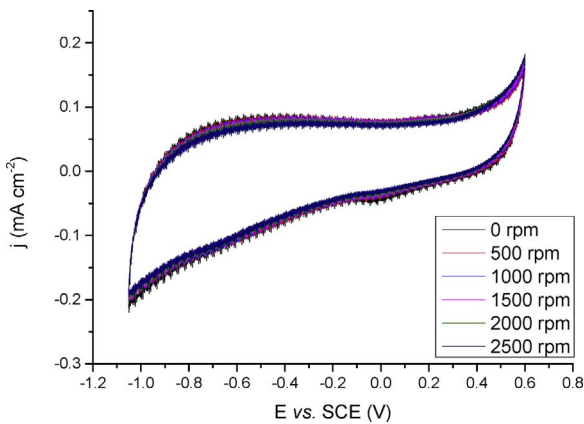


**Fig. 7.** CV experiments on glassy carbon electrode at different rotation rates (0–2500 rpm) of the rotating disk electrode ( $100 \text{ mV s}^{-1}$ ):  $0.1 \text{ M NaOH} + 0.001 \text{ M Na}_2\text{B}_{12}\text{H}_{12}$ .

to adverse poisoning effects (as for platinum, but possibly not by the same intermediates). The inability of gold to generate any current below  $-0.2 \text{ V}$  vs. SCE suggests that either  $\text{B}_{12}\text{H}_{12}^{2-}$  does not partially dissociate on gold as it does for platinum and/or that gold cannot valorize the  $\text{H}_{\text{ads}}$  possibly formed in the process (and indeed, gold has no activity towards the oxidation of  $\text{H}_{\text{ads}}$  and  $\text{H}_2$ ). To be more specific, the cyclic voltammogram can be accounted for by the Langmuir-Hinshelwood stripping of adsorbed species (likely  $\text{B}_x\text{H}_y$  compounds) as soon as surface hydroxide species are nucleated at gold. Besides, the product of this stripping would have the propensity to be electro-oxidized and desorb from the electrode surface, therefore explaining the decreased oxidation current with the revolution rate of the gold RDE and the

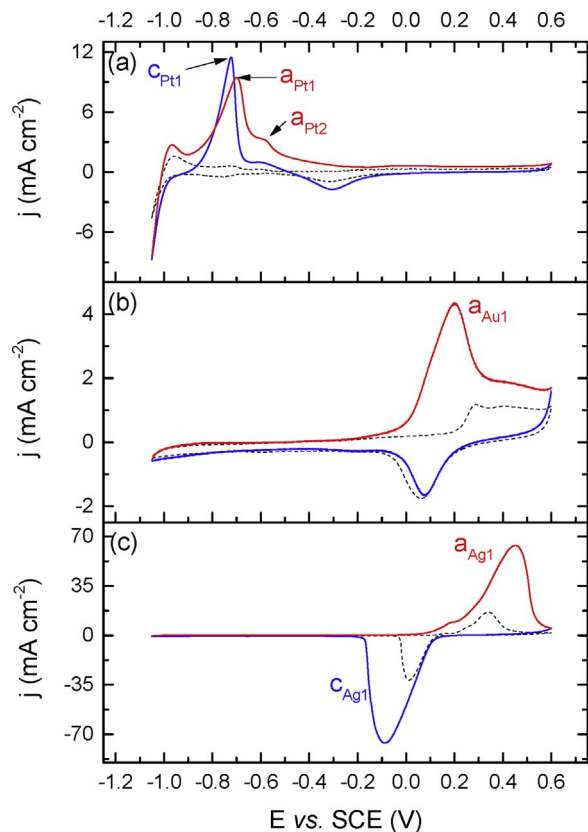


**Fig. 8.** Cyclic voltammograms obtained on platinum (a), gold (b) and silver (c) at  $100 \text{ mV s}^{-1}$  and at natural diffusion conditions (0 rpm). For each electrode, the voltammogram of  $0.1 \text{ M NaOH}$  (dashed lines) is superimposed to that of  $0.1 \text{ M NaOH} + 0.001 \text{ M Na}_2\text{B}_{12}\text{H}_{12}$  (solid lines). The red line indicates the forward sweep and the blue line the backward sweep. (For interpretation of the references to colour in this figure legend, the reader is referred to the web version of this article.)

quasi-inexistent reduction current during the negative-going sweep potential scan (in these cases, the stripping products would have the time/propensity to be expelled from the electrode surface by diffusion-convection or simple diffusion). As for platinum, gold is not an optimized catalyst for the oxidation of  $\text{B}_{12}\text{H}_{12}^{2-}$ .

With the silver electrode, the cyclic voltammogram (Fig. 8c) shows one oxidation ( $a_{\text{Ag}1}$  peaking at  $+0.45 \text{ V}$  vs. SCE) during the forward step (again likely promoted by surface (hydr)oxides formation) and one reduction peak on the backward sweep ( $c_{\text{Ag}1}$  at  $-0.09 \text{ V}$  vs. SCE), the latter implying that the oxidation process is (at least in part) reversible on bulk silver electrodes. The current density of  $a_{\text{Ag}1}$  is much higher than that shown by the other electrodes, with  $63.7 \text{ mA cm}^{-2}$ . This would suggest that a direct and possibly more complete oxidation of  $\text{B}_{12}\text{H}_{12}^{2-}$  is possible on silver, but the reaction takes place at too positive potential to hold any interest for an application in a fuel cell anode. The effect of the rotation rate of the rotating disk electrode is not detrimental in the case of the silver electrode (Fig. S3). There is even a slight increase of the current density from  $63.7 \text{ mA cm}^{-2}$  at 0 rpm to  $69.7 \text{ mA cm}^{-2}$  at 2500 rpm, which shows that silver is less affected by poisoning from adsorbed intermediates of the  $\text{B}_{12}\text{H}_{12}^{2-}$  oxidation. In any case, the very different behavior of the silver electrode in comparison to the gold electrode suggests that the oxidation of  $\text{B}_{12}\text{H}_{12}^{2-}$  involves intermediates/products which remain adsorbed at the electrode surface (one could speculate that species of the type  $\text{Ag}(\text{O}_x\text{H}_y\text{B}_z)$  form, and partly passivate the surface of the silver electrode). In this case, the redox processes would be much less limited by the charge transfer at the interface, and slightly by mass-transfer kinetics in the electrolyte.

Whatever the validity of the tentative mechanisms of  $\text{B}_{12}\text{H}_{12}^{2-}$

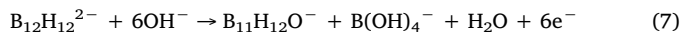
**Table 1**

Summary of the MS results with the list of the  $m/z$  values that were found on the spectrographs, the associated species, and the results for each bulk electrode (platinum, gold, silver). The  $m/z$  values corresponding to  $\text{B}_{12}\text{H}_{12}^{2-}$  has not been reported. The relative importance of each is given with ● as very minor product, ●● as minor product, ●●● as major product, ●●●● as predominant product, and × for not present.

$m/z$ values	Associated species	Platinum electrode	Gold electrode	Silver electrode
82.2	$\text{B}_7\text{H}_8^-$	×	●	×
98.1	$\text{B}_7\text{H}_8\text{O}^-$	●●●●	×	●●●●
101.2	$\text{B}_7\text{H}_{11}\text{O}^-$	●●●●	●●	●●●
110.2	$\text{B}_9\text{H}_{15}^-$	×	●●●●	×
117	$\text{B}_{10}$ -based (?)	●●	×	●●
141.2	$\text{B}_{11}\text{H}_8\text{O}^-$	●●	×	●●
145.2	$\text{B}_{11}\text{H}_{12}\text{O}^-$	●	×	●
163.2	$\text{B}_{11}\text{H}_{11}\text{O}(\text{OH})^-$	●●●●	●●	●●●●

oxidation proposed above, the aforementioned bulk electrodes can be ranked in terms of electrochemical activity (*i.e.* current density). In the present conditions, the best one is bulk silver. However, for both silver and gold, oxidation takes place at high potentials, which is irrelevant for any fuel cell applications (from that prospect, platinum is a better catalyst). Moreover, for the three electrocatalysts, the state of surface plays a big role: platinum-oxides show no activity (on the contrary to bare Pt surfaces), whereas for gold and silver, the oxidation of  $\text{B}_{12}\text{H}_{12}^{2-}$  only takes place in the metal-oxide region. This evidences the importance of surface (hydr)oxides in direct oxidation of boron hydrides like  $\text{B}_{12}\text{H}_{12}^{2-}$ . Further works should be focused on multimetallic electrodes with the objective to decrease the oxidation potential of  $\text{B}_{12}\text{H}_{12}^{2-}$  and increase its conversion to reach complete oxidation.

The oxidation products in the electrolytes were tentatively analyzed by  $^{11}\text{B}$  NMR. No signal except that of the anion  $\text{B}_{12}\text{H}_{12}^{2-}$  was observed because of too low concentrations of any oxidation intermediates or products. Alternatively, mass spectrometry was used. For each electrode, the voltammetry experiments were repeated. The potential was positively scanned from  $-1.05$  to  $+0.6$  V vs. SCE (no reverse scan) for 1000 cycles. Every 100 cycles 1 mL of the electrolyte was sampled for analysis by mass spectrometry. Several  $m/z$  values were found. The results are summarized in Table 1. The attribution of a possible product to each  $m/z$  value was done on the basis of the literature reporting stable/existing polyboranes [45–51]; however, this was not possible for all of the  $m/z$  values and the presence of other unknown species cannot be discarded. Big anion forming by one-electron electrochemical oxidation like the “dimer” of  $\text{B}_{12}\text{H}_{12}^{2-}$ , namely  $\text{B}_{24}\text{H}_{23}^{3-}$  [36], was not found in our conditions. The chemical composition of the electrolyte is complex whatever the nature of the electrode. The electrolyte composition appears to be similar for the platinum and silver electrodes. It is mainly composed to  $\text{B}_7$ - and  $\text{B}_{11}$ -based products, suggesting a partial oxidative degradation of the anion  $\text{B}_{12}\text{H}_{12}^{2-}$  [35]. The formation of two of the identified species may be proposed to take place as follows. One may first envisage the partial oxidative degradation of  $\text{B}_{12}\text{H}_{12}^{2-}$  into  $\text{B}_{11}\text{H}_{12}\text{O}^-$ :



However, the amount of  $\text{B}_{11}\text{H}_{12}\text{O}^-$  in the analyzed electrolyte samples is low whereas that of  $\text{B}_{11}\text{H}_{12}\text{O}(\text{OH})^-$  is much higher; the occurrence of an equilibrium between these two acid-base species is secondly possible (with predominance of the latter form):



With respect to the other predominant product,  $\text{B}_7\text{H}_{11}\text{O}^-$ , it may directly form from  $\text{B}_{12}\text{H}_{12}^{2-}$  or from a  $\text{B}_{11}$ -based intermediate. The same hypotheses apply to the other products. With respect to the gold electrode, the oxidation path is, to some extent, different since the nature of the products is partly different. The occurrence of the reactions (7) and (8) is here also likely, but there is another more important

(direct or stepwise) path leading to  $\text{B}_9\text{H}_{15}$ . In fact, the main conclusion that can be made from these results is that the oxidation of  $\text{B}_{12}\text{H}_{12}^{2-}$  over the bulk electrodes investigated here is complex and only partial.

#### 4. Conclusion

The oxidation of the highly stable aqueous solution of sodium decahydro-closo-dodecaborate  $\text{Na}_2\text{B}_{12}\text{H}_{12}$  has been studied with platinum, gold and silver electrodes. Prior the cyclic voltammetry experiments, it was ensured that: (i)  $\text{Na}_2\text{B}_{12}\text{H}_{12}$  was successfully synthesized (as characterized by NMR, FTIR, XRD, and Raman spectroscopy); (ii) it is thermally stable up to 100 °C (as evidenced by TGA and DSC); and (iii) it is chemically stable in both acidic and basic media. The occurrence of acid-catalyzed hydrolysis was not observed over a period of 3 weeks. In parallel, the absence of heterogeneous hydrolysis was verified by DEMS, with a gold electrode. Both of these experiments confirmed the chemical stability of the aqueous solution of  $\text{Na}_2\text{B}_{12}\text{H}_{12}$ .

The oxidation of the  $\text{B}_{12}\text{H}_{12}^{2-}$  anion was found to take place over each of the electrodes even though the processes differ with the nature of the metal at stake. With platinum, the oxidation occurs at potential values which are just positive to the hydrogen reversible potential. On the contrary, with the other electrodes, it happens at much more positive potential values. In that latter case, fuel cell application may not be possible (the anode would then operate at a potential close to that of a practical cathode, thereby leading to near-zero cell voltage), so the best option as anode catalyst amongst the three investigated metals would be platinum. However, the oxidation is not complete with this electrode (neither is it with gold and silver), and an optimized electrocatalyst is yet to be found.

The oxidation products over 1000 cycles were analyzed by mass spectrometry. It was found the presence of several products, all containing less than 12 boron atoms. Although the identification was difficult for few  $m/z$  values, the results suggest the formation of  $\text{B}_{11}$ - and  $\text{B}_7$ -based products mainly. An example of product is  $\text{B}_{11}\text{H}_{12}\text{O}^-$ , which would form by partial oxidative degradation of  $\text{B}_{12}\text{H}_{12}^{2-}$ . Whatever the nature of the electrode, the composition of the used anolytes was complex, consistently with the apparently complex oxidation of the highly stable  $\text{B}_{12}\text{H}_{12}^{2-}$ .

#### Acknowledgments

UBD and SOA thank the ANR (Agence Nationale de la Recherche), the program “Investissements d’Avenir” with the reference ANR-10-LABX-05-01 (LabEx CheMISyst), and the Région Languedoc-Roussillon for the program “Chercheur(se)s d’Avenir 2013” (project C3/2013 008555). MC thanks the French IUF for funding. AZ thanks the region Rhône-Alpes for funding his PhD (grant ARC Energie 2013).

#### Appendix A. Supplementary data

Supplementary data associated with this article can be found, in the online version, at <http://dx.doi.org/10.1016/j.apcatb.2017.09.068>.

#### References

- [1] E.H. Yu, X. Wang, U. Krewer, L. Li, K. Scott, Energy Environ. Sci. 5 (2012) 5668–5680.
- [2] Y. Zhu, N.S. Hosmane, Coord. Chem. Rev. 293–294 (2015) 357–367.
- [3] M.M. Kreevoy, J.E.C. Hutchins, J. Am. Chem. Soc. 94 (1972) 6371–6376.
- [4] K.N. Mochalov, V.S. Khain, G. Gilmansh, Doklady Akademii Nauk SSSR 162 (1965) 613–616.
- [5] M.M. Kreevoy, R.W. Jacobson, Ventron Alembic 15 (1979) 2–3.
- [6] R.L. Pecsok, J. Am. Chem. Soc. 75 (1953) 2862–2864.
- [7] W.H. Stockmayer, D.W. Rice, C.C. Stephenson, J. Am. Chem. Soc. 77 (1955) 1980–1983.
- [8] F.H.B. Lima, A.M. Pasqualetti, M.B. Molina Concha, M. Chatenet, E.A. Ticianelli, Electrochim. Acta 84 (2012) 202–212.
- [9] I. Merino-Jiménez, C. Ponce De León, A.A. Shah, F.C. Walsh, J. Power Sources 219 (2012) 339–357.

- [10] M.C.S. Escaño, R.L. Arevalo, E. Gyenge, H. Kasai, *J. Phys. Cond. Matter* 26 (2014) 353001.
- [11] P.Y. Olu, N. Job, M. Chatenet, *J. Power Sources* 327 (2016) 235–257.
- [12] J.P. Elder, A.H. Hickling, *Trans. Faraday Soc.* 58 (1962) 1852–1864.
- [13] U. Sanyal, U.B. Demirci, B.R. Jagirdar, P. Miele, *ChemSusChem.* 4 (2011) 1731–1739.
- [14] X.B. Zhang, S. Han, J.M. Yan, M. Chandra, H. Shioyama, K. Yasuda, N. Kuriyama, T. Kobayashi, Q. Xu, *J. Power Sources* 168 (2007) 167–171.
- [15] L.C. Nagle, J.F. Rohan, *J. Electrochem. Soc.* 153 (2006) C773–C776.
- [16] X.B. Zhang, S. Han, J.M. Yan, H. Shioyama, N. Kuriyama, T. Kobayashi, Q. Xu, *Int. J. Hydrogen Energy* 34 (2009) 174–179.
- [17] M.B. Molina Concha, M. Chatenet, F.H.B. Lima, E.A. Ticianelli, *Electrochim. Acta* 89 (2013) 607–615.
- [18] P.Y. Olu, F. Deschamps, G. Caldarella, M. Chatenet, N. Job, *J. Power Sources* 297 (2015) 492–503.
- [19] A. Zadick, L. Dubau, K. Artyushkova, A. Serov, P. Atanassov, M. Chatenet, *Nano Energy* 37 (2017) 248–259.
- [20] A.K. Figen, M.B. Piskin, B. Coşkuner, V. İmamoğlu, *Int. J. Hydrogen Energy* 38 (2013) 16215–16628.
- [21] S. Pylypko, A. Zadick, M. Chatenet, P. Miele, M. Cretin, U.B. Demirci, *J. Power Sources* 286 (2015) 10–17.
- [22] T.Q. Hua, R.K. Ahluwalia, *Int. J. Hydrogen Energy* 37 (2012) 14382–14392.
- [23] R.N. Grimes, *J. Chem. Educ.* 81 (2004) 657–672.
- [24] I.B. Sivaev, V.V. Bregadze, *Eur. J. Inorg. Chem.* (2009) 1433–1450.
- [25] A.V. Safronov, S.S. Jalilatgi, H.B. Lee, M.F. Hawthorne, *Int. J. Hydrogen Energy* 36 (2011) 234–239.
- [26] L. He, H.W. Li, S.J. Hwang, E. Akiba, *J. Phys. Chem.* 118 (2014) 6084–6089.
- [27] A. Yu. Bykov, N.B. Mal'tseva, K. Yu. Zhizhin, N.T. Kuznetsov, *Russ. J. Inorg. Chem.* 58 (2013) 1321–1323.
- [28] M. Chatenet, F.H.B. Lima, E.A. Ticianelli, *J. Electrochem. Soc.* 157 (2010) B697–B704.
- [29] S.J. Hwang, R.C. Bowman, J.W. Reiter Jr., J. Rijssenbeek, G.L. Soloveichik, J.C. Zhao, H. Kabbour, C.C. Ahn, *J. Phys. Chem. C* 112 (2008) 3164–3169.
- [30] S.R. Ghanta, M.H. Rao, K. Muralidharan, *Dalton Trans.* 42 (2013) 8420–8425.
- [31] X. Chen, H.K. Lingam, Z. Huang, T. Yisgedu, J.C. Zhao, S.G. Shore, *J. Phys. Chem. Lett.* 1 (2010) 201–204.
- [32] J.H. Her, W. Zhou, V. Stavila, C.M. Brown, T.J. Udovic, *J. Phys. Chem.* 113 (2009) 11187–11189.
- [33] N. Verdal, J.H. Her, V. Stavila, A.V. Soloninin, O.A. Babanova, A.V. Skripov, T.J. Udovic, J.J. Rush, *J. Solid State Chem.* 2014 (2012) 81–91.
- [34] E.L. Muetterties, J.H. Balthis, Y.T. Chia, W.H. Knuth, H.C. Miller, *Inorg. Chem.* 3 (1964) 444–451.
- [35] A. Kaczmarczyk, G.B. Kolski, W.P. Townsend, *J. Am. Chem. Soc.* 87 (1965) 1413–1413.
- [36] R.J. Wiersema, R.L. Middaugh, *Inorg. Chem.* 8 (1969) 2074–2079.
- [37] O. Volkov, P. Paetzold, C. Hu, *Z. Anorg. Allg. Chem.* 632 (2006) 945–948.
- [38] M.B. Molina Concha, M. Chatenet, *Electrochim. Acta* 54 (2009) 6110–6129.
- [39] P.Y. Olu, C. Barros, N. Job, M. Chatenet, *Electrocatalysis* 5 (2014) 288–300.
- [40] R. Ojani, R. Valiollahi, J.B. Raoof, *Appl. Surf. Sci.* 311 (2014) 245–251.
- [41] P.Y. Olu, A. Bonnefont, M. Rouhet, S. Bozdech, N. Job, M. Chatenet, E. Savinova, *Electrochim. Acta* 179 (2015) 637–646.
- [42] Z. Jusys, R.J. Behm, *Electrochim. Commun.* 60 (2015) 9–12.
- [43] P.-Y. Olu, C. Barros, N. Job, M. Chatenet, *Electrocatalysis* 5 (2014) 288–300.
- [44] D.A. Finkelstein, C.D. Letcher, D.J. Jones, L.M. Sandberg, D.J. Watts, H.D. Abruna, *J. Phys. Chem. C* 117 (2013) 1571–1581.
- [45] A.B. Burg, R. Kratzer, *Inorg. Chem.* 1 (1962) 725–730.
- [46] J. Dobson, P.C. Keller, R. Schaeffer, *Inorg. Chem.* 3 (1968) 399–402.
- [47] R.J. Remmel, H.D. Johnson, L.S. Jaworowsky, S.G. Shore, *J. Am. Chem. Soc.* 97 (1975) 5395–5403.
- [48] R.E. Williams, *Chem. Rev.* 92 (1992) 177–207.
- [49] H. Beall, D.F. Gaines, *Inorg. Chim. Acta* 289 (1999) 1–10.
- [50] R.B. King, *Inorg. Chem.* 40 (2001) 6369–6374.
- [51] F. Schlüter, E. Bernhardt, *Inorg. Chem.* 50 (2011) 2580–2589.